(zeroth-order Bessel function) affects the field distribution of this resonance.

In the case of the square ferrite planar resonator, the magnetic tuning characteristics and the instantaneous relative electric field intensities across the resonator are shown in Figs. 8 and 9 (a), (b), and (c), respectively. It is found from the figures that almost the same resonant characteristics as obtained for a triangular resonator result.

V. Conclusion

The analysis given can be applied to cylindrical cavities with arbitrarily shaped, longitudinally magnetized ferrite posts as well as to arbitrarily shaped, ferrite planar resonators or circuits. The numerical results obtained for all the examples are found to be in agreement with the experimental results and the previously published experimental ones. The point-matching technique will be useful in the design and analysis of ferrite planar circuits as well as magnetically tunable cavities.

References

[1] G. S. Heller and B. Lax, "Use of perturbation theory for cavities and waveguides containing ferrite," *IRE Trans. Antennas Propagat.*, vol. 4, p. 584, Mar. 1956.

[2] G. S. Heller, "Ferrite loaded cavity resonators," *Onde Elec., Spec. Suppl.*, p. 588, Oct. 1957.

[3] H. E. Bussey and L. A. Steinert, "An exact solution for a cylindrical cavity containing a gyromagnetic material," *Proc. IRE*, vol. 45, p. 693, 1957.

[4] H. Gamo, "The Faraday rotation of waves in a circular waveguide," *J. Phys. Soc.* (Japan), vol. 8, p. 176, 1953.

[5] M. L. Kales, "Modes in waveguides containing ferrite," *J. Appl. Phys.*, vol. 24, p. 604, 1953.

[6] H. Brand, "Uber elektromagnetische Eigenschwingungen quaderfömiger Ferritresonatoren," thesis, Technical University Aachen, 1962.

[7] D. M. Bolle, "Ferrite loaded rectangular cavities," *Electron. Lett.*, vol. 2, no. 1, pp. 17–18, Jan. 1966.

[8] L. Lewin and E. D. Nielsen, "On the inadequacy of discrete mode-matching techniques in some waveguide discontinuity problems," *IEEE Trans. Microwave Theory Tech.*, vol. MTT-18, pp. 364–372, July 1970.

[9] L. Lewin, "On the restricted validity of point-matching techniques," *IEEE Trans. Microwave Theory Tech.*, vol. MTT-18, pp. 1041–1047, Dec. 1970.

[10] T. Miyoshi, S. Yamaguchi, and S. Goto, "Ferrite planar circuits in microwave integrated circuits," *IEEE Trans. Microwave Theory Tech.*, vol. MTT-25, pp. 593–600, July 1977.

[11] T. Okoshi and T. Miyoshi, "The planar circuit—An approach to microwave integrated circuitry," *IEEE Trans. Microwave Theory Tech.*, vol. MTT-20, pp. 245–252, Apr. 1972.

[12] S. A. Schelkunoff, *Electromagnetic Waves*. New York: Van Nostrand, 1943, pp. 392–397.

[13] I. Wolff, *Fields and Waves in Gyrotropic Microwave Structures* (in German). Verlag Friedr. Vieweg+Sohn, Braunschweig, 1975.

[14] Y. Akaiwa, "Operation modes of a waveguide *Y* circulator," *IEEE Trans. Microwave Theory Tech.*, vol. MTT-22, pp. 954–960, Nov. 1974.

[15] ——, "Mode classification of a triangular ferrite post for *Y* circulator operation," *IEEE Trans. Microwave Theory Tech.*, vol. MTT-25, pp. 59–61, Jan. 1977.

[16] I. Wolff and N. Knoppik, "Rectangular and circular microstrip disk capacitors and resonators," *IEEE Trans. Microwave Theory Tech.*, vol. MTT-22, pp. 857–864, Oct. 1974.

[17] B. Lax and K. J. Button, *Microwave Ferrites and Ferrimagnetics*. New York: Lincoln Laboratory Publications, McGraw-Hill, 1962, pp. 418–420.

[18] J. Helszajn and D. S. James, "Planar triangular resonators with magnetic walls," *IEEE Trans. Microwave Theory Tech.*, vol. MTT-26, pp. 95–100, Feb. 1978.

Theory of Infrared and Optical Frequency Amplification in Metal–Barrier–Metal Diodes

DAVID M. DRURY AND T. KORYU ISHII, SENIOR MEMBER, IEEE

***Abstract*—The near-infrared and optical frequency power gain of a metal–barrier–metal (MBM) point contact diode exhibiting a negative differential resistance region in its current–voltage characteristic is derived as a function of frequency. The diode is treated as a traveling-wave amplifier. The starting point for the analysis is the known electric and magnetic field distribution of the surface waves that propagate in the oxide barrier layer between the diode whisker and substrate, assuming no tunneling current is present. Then the differential tunneling conductance is introduced, and the electric and magnetic field distribution is used to find the propagation constant of the equivalent transmission line formed by the diode structure. It is shown that if the differential tunneling conductance is negative, gain can result. It is shown theoretically that the diode amplifier can provide approximately a 6-dB gain from the CO_2 laser frequency to the He–Ne laser frequency.**

Manuscript received April 24, 1978; revised January 9, 1979.

D. M. Drury was with the Department of Electrical Engineering, Marquette University, Milwaukee, WI 53233. He is now with Sandia Laboratories, Albuquerque, NM 87185.

T. K. Ishii is with the Department of Electrical Engineering, Marquette University, Milwaukee, WI 53233.

0018-9480/79/0600-0598$00.75 ©1979 IEEE

I. Introduction

THE FREQUENCY response of metal–barrier–metal (MBM) diodes has been shown to extend into the optical range [1], [2]. Some MBM diodes have been shown to have a negative differential resistance region in their $I-V$ characteristics [3], [4]. It has been suggested that the combination of optical frequency performance and negative differential resistance could produce infrared or optical frequency amplification in an MBM diode [3]. However, the theoretical details of the amplification mechanism have not been published. The object of this paper is to present a theory of infrared and optical frequency amplification in an MBM diode.

As shown below, the point contact MBM diode is treated as a traveling-wave amplifier at near-infrared or optical frequencies due to the short wavelength of the surface plasma oscillations by which the signal is coupled to the diode. A simplified model of an MBM diode amplifier is analyzed by treating the tunneling surfaces of the diode as a transmission line. This analysis shows that the proposed amplifier would have a much wider useful bandwidth than would a laser amplifier.

II. Theoretical Analysis

At millimeter and far-infrared frequencies, the coupling of incident radiation to the whisker of a point contact MBM diode can be described by the classical antenna theory [5]. However, the classical antenna theory fails at near-infrared and optical frequencies, where the incident radiation couples to the whisker by inducing surface waves on the whisker [6]. These surface waves in turn can induce surface waves that propagate through the thin oxide layer that separates the whisker from the metal substrate [6]. In the opinion of the authors, these "gap modes" can produce amplification of infrared and optical waves through interaction with the tunneling current.

A schematic diagram of an idealized MBM diode structure is shown in Fig. 1. To simplify the analysis, the whisker is assumed to have a rectangular, rather than a circular, cross section of length $2a$ in the z direction and width $2b$ in the y direction. The thickness of the oxide layer through which the diode current tunnels in the x direction is $2d$. Electromagnetic fields in the oxide layer were calculated using similar assumptions and approaches used by Economou [7]. Assuming that the tunneling electrons do not greatly perturb the modes of the electromagnetic fields of the structure, and assuming that $d/dy \to 0$ (two-dimensional model) to simplify the analysis, with the aid of [7] the fields in the oxide layer can be shown to be

$$E_x = E_0\left(G_1 e^{\delta_b x} - G_2 e^{-\delta_b x}\right) \tag{1}$$

$$E_z = -jE_0\frac{\delta_b}{k}\left(G_1 e^{\delta_b x} + G_2 e^{-\delta_b x}\right) \tag{2}$$

and

$$H_y = E_0\frac{\omega\epsilon_b}{k}\left(G_1 e^{\delta_b x} - G_2 e^{-\delta_b x}\right) \tag{3}$$

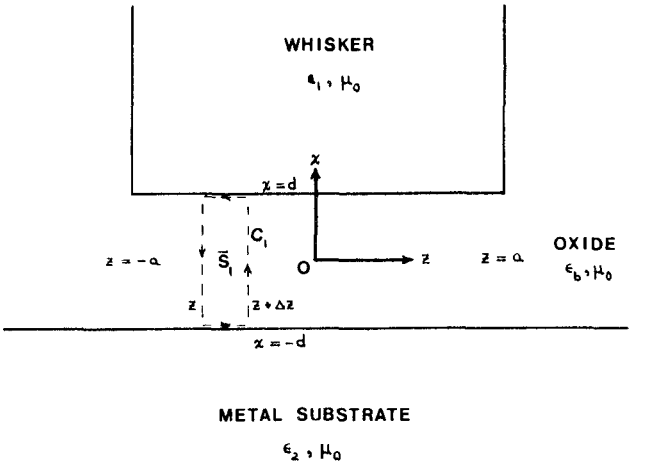

Fig. 1. The idealized metal–barrier–metal (MBM) diode structure, showing the path of integration C_1 used to determine the resistance per unit length and inductance per unit length of the equivalent transmission line.

where

$$G_1 = \frac{1}{2}\left(1 - \frac{\epsilon_1\delta_b}{\epsilon_b\delta_1}\right)e^{-\delta_b d} \tag{4}$$

$$G_2 = \frac{1}{2}\left(1 + \frac{\epsilon_1\delta_b}{\epsilon_b\delta_1}\right)e^{\delta_b d} \tag{5}$$

$$\delta_{b,1,2}^2 = k^2 - \omega^2\mu_0\epsilon_{b,1,2} \tag{6}$$

and all fields are understood to be multiplied by $e^{j(\omega t - kz)}$ for propagation in the positive z direction. The permittivity of the oxide layer is $\epsilon_b = \epsilon_r\epsilon_0$, while ϵ_1 is the frequency dependent permittivity of the metal in the region $x > d$. Both metals and the oxide are assumed to be nonmagnetic, i.e., $\mu = \mu_0$ in all three regions [7]. Note that E_y, H_x, and H_z are identically zero; the gap mode is a TM mode [7].

Since (1)–(6) were derived neglecting the presence of tunneling electrons, these equations do not show amplification. Using a method of analysis given by Jordan and Balmain [8], (1)–(6) will be used to find the parameters of the transmission line formed by the metal surfaces at $x = \pm d$. (In [8], the method of analysis assumed that the fields did not penetrate the surface of the metal. In the situation considered in this paper, the fields do penetrate into the metals. However, as is shown in the Appendix, the method described in [8] can be applied to this case as well.) The differential tunneling conductance per unit length in the z direction of the MBM diode will be included when finding the transmission line parameters, so that the resulting propagation constant of the transmission line will show the amplification of the wave.

Integrating Maxwell's equation for the curl of the electric field over the surface $\bar{S}_1$, where $\bar{S}_1$ is the oriented surface enclosed by the curve C_1 shown in Fig. 1, gives

$$\int_{S_1}(\bar{\nabla}\times\bar{E})\cdot d\bar{S} = -j\omega\mu_0\int_{S_1}\bar{H}\cdot d\bar{S}$$

which becomes, after applying Stoke's theorem,

$$\oint_{C_1} \bar{E}\cdot d\bar{l} = -j\omega\mu_0 \int_{S_1} \bar{H}\cdot d\bar{S}. \tag{7}$$

The left side of this equation can be expanded into

$$\oint_{C_1} \bar{E}\cdot d\bar{l} = \int_{-d}^{d} E_x\Big|_{z=z+\Delta_z} dx + \int_{z+\Delta z}^{z} E_z\Big|_{x=d} dz + \int_{d}^{-d} E_x\Big|_{z=z} dx + \int_{z}^{z+\Delta z} E_z\Big|_{x=-d} dz. \tag{8}$$

Substituting from (1) and (2) into (8), and carrying out the indicated integrations by defining

$$-\Delta V = \int_{-d}^{d} E_x\Big|_{z=z+\Delta z} dx + \int_{d}^{-d} E_x\Big|_{z=z} dx$$

and by making the approximation

$$\int_{z}^{z+\Delta z} e^{-jkz} dz = -\int_{z+\Delta z}^{z} e^{-jkz} dz \cong e^{-jkz}\Delta z \tag{9}$$

for Δz much less than one wavelength gives

$$\int_{C_1} \bar{E}\cdot d\bar{l} = -\Delta V + j2E_0 \frac{\delta_b}{k}(G_1 - G_2)\sinh(\delta_b d)e^{-jkz}\Delta z. \tag{10}$$

Substituting (3) into the right side of (7) yields

$$-j\omega\mu_0 \int_{S_1} \bar{H}\cdot d\bar{S} = -jE_0 \frac{\omega^2\mu_0\epsilon_b}{k} \int_{z}^{z+\Delta z}\int_{-d}^{d} (G_1 e^{\delta_b x} - G_2 e^{-\delta_b x}) e^{-jkz} dx dz = -2jE_0 \frac{\omega^2\mu_0\epsilon_b}{k\delta_b}(G_1 - G_2)\sinh(\delta_b d)e^{-jkz}\Delta z. \tag{11}$$

Substituting (10) and (11) into (7), combining terms, and using (6) produces

$$\Delta V = 2jE_0 \frac{k}{\delta_b}(G_1 - G_2)\sinh(\delta_b d)e^{-jkz}\Delta z. \tag{12}$$

This equation is still not in the form of a transmission line equation, since it contains the electric field magnitude E_0. To eliminate this constant, define the transmission line current I as

$$I = -2bH_y\big|_{x=d} \tag{13}$$

(see the Appendix for the validity of this equation) which becomes, after substituting (3),

$$I = -\frac{2b\omega\epsilon_b E_0}{k}\left(G_1 e^{\delta_b d} - G_2 e^{-\delta_b d}\right)e^{-jkz}.$$

Solving this equation for $E_0 e^{-jkz}$ and substituting in (12) gives

$$\frac{\Delta V}{\Delta z} = -j\frac{k^2(G_1 - G_2)\sinh(\delta_b d)}{b\omega\epsilon_b\delta_b\left(G_1 e^{\delta_b d} - G_2 e^{-\delta_b d}\right)} I. \tag{14}$$

By defining

$$R + j\omega L = j\frac{k^2(G_1 - G_2)\sinh(\delta_b d)}{b\omega\epsilon_b\delta_b\left(G_1 e^{\delta_b d} - G_2 e^{-\delta_b d}\right)} \tag{15}$$

where R is the resistance per unit length of the transmission line, and L is the inductance per unit length, (14) is shown to have the exact form of a conventional transmission line equation [8].

Introducing the tunneling current density $\bar{J}_t$ into Maxwell's equation for the curl of the magnetic field and integrating over the oriented surface enclosed by the curve C_2, shown in Fig. 2, gives

$$\int_{S_2} (\bar{\nabla}\times\bar{H})\cdot d\bar{S} = \int_{S_2} \left[\bar{J}_t + j\omega\epsilon_b \bar{E}\big|_{x=d}\right]\cdot d\bar{S}. \tag{16}$$

Applying Stoke's theorem and substituting (13) into the left side of (16) results in

$$\int_{S_2} (\bar{\nabla}\times\bar{H})\cdot d\bar{S} = \oint_{c_2} \bar{H}\cdot d\bar{l} = -2b\left(H_y\big|_{z+\Delta z} - H_y\big|_z\right) = \Delta I. \tag{17}$$

Let g_t designate the differential tunneling conductance per unit length, which can be determined from the static current–voltage characteristic of the diode. Then

$$\int_{S_2} \bar{J}_t\cdot d\bar{S} = -g_t V\Delta z. \tag{18}$$

Furthermore,

$$j\omega\epsilon_b \int_{S_2} \bar{E}\big|_{x=d}\cdot d\bar{S} = j2b\omega\epsilon_b E_0\left(G_1 e^{\delta_b d} - G_2 e^{-\delta_b d}\right)e^{-jkz}\Delta z \tag{19}$$

where (1) and (9) have been used. Define the transmission line voltage as

$$V = -\int_{-d}^{d} E_x dx.$$

Substituting from (1) and integrating gives

$$V = -2\frac{E_0}{\delta_b}(G_1 - G_2)\sinh(\delta_b d)e^{-jkz}.$$

The result of solving this equation for $E_0 e^{-jkz}$ and substituting the result in (19) is

$$j\omega\epsilon_b \int_{S_2} \bar{E}\big|_{x=d}\cdot d\bar{S} = -j\frac{b\omega\epsilon_b\delta_b\left(G_1 e^{\delta_b d} - G_2 e^{-\delta_b d}\right)}{(G_1 - G_2)\sinh(\delta_b d)} V\Delta z.$$

Substituting this equation, (17), and (18) into (16) results in

$$\frac{\Delta I}{\Delta z} = -\left[g_t + j\frac{b\omega\epsilon_b\delta_b\left(G_1 e^{\delta_b d} - G_2 e^{-\delta_b d}\right)}{(G_1 - G_2)\sinh(\delta_b d)}\right] V. \tag{20}$$

By defining

$$G + j\omega C = g_t + j\frac{b\omega\epsilon_b\delta_b\left(G_1 e^{\delta_b d} - G_2 e^{-\delta_b d}\right)}{(G_1 - G_2)\sinh(\delta_b d)} \tag{21}$$

where G is the conductance per unit length, and C is the capacitance per unit length of the equivalent transmission line, (20) is shown to have the form of a transmission line equation [8].

Since all of the parameters of the transmission line are now known, the propagation constant γ of the line can be found from [8]

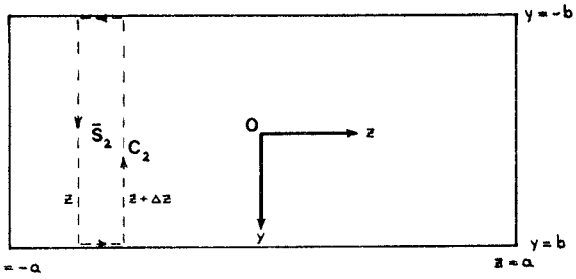

Fig. 2. Interface between metal 1 and the oxide layer at $x=d$, showing the path of integration C_2 used to determine the conductance per unit length and capacitance per unit length of the equivalent transmission line.

$$\gamma=\sqrt{(R+j\omega L)(G+j\omega C)} \tag{22}$$

where all fields are assumed to be proportional to $e^{-\gamma z}$ for propagation in the positive z direction. Substituting from (15) and (21) into (22) gives for the propagation constant:

$$\gamma=\left\{-k^2+jg_t\frac{k^2}{b\omega\epsilon_b\delta_b}\left[\frac{\epsilon_b\delta_1}{\epsilon_1\delta_b}\sinh(\delta_b d)+\cosh(\delta_b d)\right]\sinh(\delta_b d)\right\}^{1/2} \tag{23}$$

where G_1 and G_2 have been eliminated with the aid of (4) and (5).

In practice, losses in the system—which can become quite large as the frequency approaches the surface-wave resonant frequency of one of the metals [9]—cause ϵ_1, ϵ_b, k, and δ_b to become complex. However, it has been shown [7] that in the frequency range of interest the permittivities of the metals can be considered to be real. Therefore, the permittivity of the oxide layer will also be assumed to be real. With no losses in the material, k and δ_b are also real. In the case of similar metals, i.e., $\epsilon_1=\epsilon_2$, it can be shown [6], [7] that

$$\frac{\epsilon_b\delta_1}{\epsilon_1\delta_b}=-\tanh(\delta_b d). \tag{24}$$

With this substitution, (23) reduces to

$$\gamma=\left[-k^2+jg_t\frac{k^2\tanh(\delta_b d)}{b\omega\epsilon_b\delta_b}\right]^{1/2}. \tag{25}$$

In most MBM diodes of interest, the gap $2d$ between the upper and lower metal surfaces is less than 20 Å [1], [4], [10]. As will be shown below, in the frequency range of interest $\delta_b d\ll 1$, and $\tanh(\delta_b d)\cong\delta_b d$. With this final substitution, (25) reduces to

$$\gamma=k\sqrt{-1+j\frac{g_t d}{b\omega\epsilon_b}} \tag{26}$$

or, in polar form,

$$\gamma=k\left[1+\frac{g_t^2d^2}{b^2\omega^2\epsilon_b^2}\right]^{1/4}\exp\left\{\frac{j}{2}\left[\pi-\arctan\left(\frac{g_t d}{b\omega\epsilon_b}\right)\right]\right\}. \tag{27}$$

As can be seen from (27), if $g_t<0$, then $\mathrm{Re}\,(\gamma)<0$. This is one of the necessary conditions that the amplification is possible [16]. To obtain the real part of (27), note that [11]

$$\cos\left(\frac{\pi}{2}-\frac{\theta}{2}\right)=\sin\frac{\theta}{2}$$

and in this case,

$$\theta=\arctan\left(\frac{g_t d}{b\omega\epsilon_b}\right)$$

then [11]

$$\sin\frac{\theta}{2}=\frac{1}{\sqrt{2}}\left[1-\frac{1}{\sqrt{\frac{g_t^2d^2}{b^2\omega^2\epsilon_b^2}+1}}\right]^{1/2}$$

so that, for negative g_t, the power gain per unit length can be written as

$$\alpha=2\,\mathrm{Re}\,(\gamma)=\sqrt{2}\,k\left[1+\frac{g_t^2d^2}{b^2\omega^2\epsilon_b^2}\right]^{1/4}\cdot\left[1-\frac{1}{\sqrt{\frac{g_t^2d^2}{b^2\omega^2\epsilon_b^2}+1}}\right]^{1/2}$$

or

$$\alpha=\sqrt{2}\,k\left[\sqrt{\frac{g_t^2d^2}{b^2\omega^2\epsilon_b^2}+1}\;-1\right]^{1/2}. \tag{28}$$

In order to obtain α as a function of frequency, it is necessary to know the dispersion relation of the gap mode. In the case of similar metals it has been shown that the dispersion relation can be approximated by [7]

$$\omega=ck\left[\frac{d}{\epsilon_r\left(d+\frac{c}{\omega_p}\right)}\right]^{1/2}. \tag{29}$$

The gap spacing $2d$ in most MBM diodes is less than 20 Å, while the bulk plasma oscillation frequency ω_p of the metal is on the order of $10^{16}\ \mathrm{s}^{-1}$ [1]–[7], [9], [10], [13], [14]. Therefore, $c/\omega_p\gg d$, and (29) reduces to

$$\omega=k\left[\omega_p cd/\epsilon_r\right]^{1/2}. \tag{30}$$

Substituting this result in (28) produces

$$\alpha=\omega\sqrt{\frac{2\epsilon_r}{\omega_p cd}}\left[\sqrt{\frac{g_t^2d^2}{b^2\omega^2\epsilon_b^2}+1}\;-1\right]^{1/2}\quad[\mathrm{Np/m}]. \tag{31}$$

The total power gain over the length $2a$ in the z direction is

$$G=2a\alpha=2a\omega\sqrt{\frac{2\epsilon_r}{\omega_p cd}}\left[\sqrt{\frac{g_t^2d^2}{b^2\omega^2\epsilon_b^2}+1}\;-1\right]^{1/2}\quad[\mathrm{Np}]$$

or

$$G=8.69a\omega\sqrt{\frac{2\epsilon_r}{\omega_p cd}}\left[\sqrt{\frac{g_t^2d^2}{b^2\omega^2\epsilon_b^2}+1}\ -1\right]^{1/2}\quad[\text{dB}]. \tag{32}$$

It should be noted that if (30) is substituted into (6), δ_b becomes

$$\delta_b^2=\omega^2\epsilon_r\left[\frac{1}{\omega_p cd}-\frac{1}{c^2}\right].$$

With the same numerical values used in Section III below, this gives

$$\delta_b d=(1.9\times10^{-17})\omega$$

so for all values of ω less than 10^{16} s^{-1} (in other words, all frequencies of interest in this paper) $\delta_b d$ is indeed much less than unity, so the approximation leading to (26) is valid.

III. Numerical Example

Assume a point contact MBM diode with $a=b=1000$ Å and $d=5$ Å. These numbers are typical for point contact MBM structures [4]. If the diode is made of gold, then $\epsilon_r=3$ [10] and $\omega_p=1.38\times10^{16}$ s^{-1} [12]. With these values (32) becomes

$$G=(4.68\times10^{-14})\omega\left[\sqrt{(3.55\times10^{16})\frac{g_t^2}{\omega^2}+1}\ -1\right]^{1/2}. \tag{33}$$

In order to produce usable gain at the lowest frequency of interest, the CO_2 laser frequency $\omega=1.76\times10^{14}$ s^{-1}, it can be seen from (33) that g_t must have a value of approximately 1×10^6 S/m. Substituting this value into (33) gives

$$G=(4.68\times10^{-14})\omega\left[\sqrt{\frac{3.55\times10^{28}}{\omega^2}+1}\ -1\right]^{1/2}. \tag{34}$$

Equation (34) is plotted as the solid line in Fig. 3.

To the author's knowledge at the time of writing this paper, no stable negative conductance MBM device, which is stable enough to observe such amplification, has been constructed [14], [15]. Therefore, it is of value to compute gain for a wide range of possible value of the negative conductance. If g_t is assumed to be 1×10^7 S/m, then

$$(3.55\times10^{16})(g_t^2/\omega^2)\gg1$$

and (33) becomes

$$G=(2.03\times10^{-6})\sqrt{\omega}\ . \tag{35}$$

This equation is plotted as the dotted line in Fig. 3. If g_t is assumed to have a smaller value of 1×10^5 S/m, then $(3.55\times10^{16})(g_t^2/\omega^2)\ll1$, and by using the binomial expansion it can be shown that (33) takes the form

$$G=(6.24\times10^{-6})g_t=0.624\quad[\text{dB}]. \tag{36}$$

This equation is plotted as the dashed line in Fig. 3.

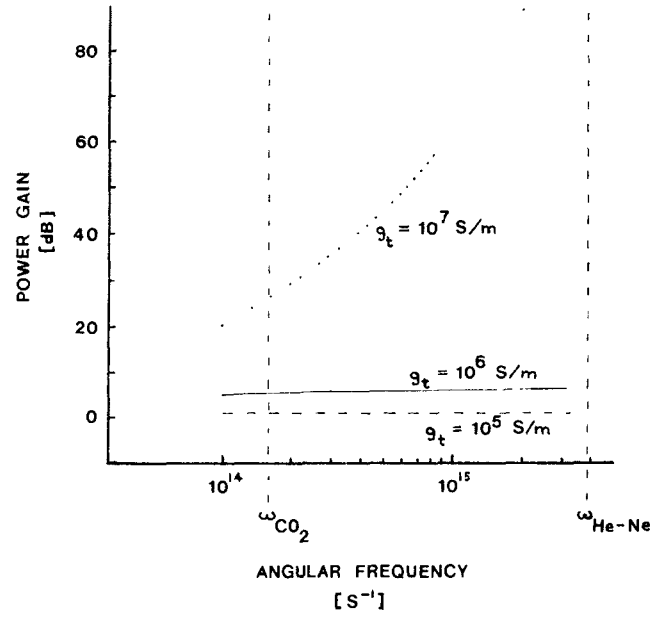

Fig. 3. Infrared and optical frequency response of an MBM diode amplifier for three different values of the diode's negative differential conductance.

Point contact MBM diodes are extremely unstable. Laboratory lifetimes of devices exhibiting negative resistance are typically measured in seconds. Fortunately, thin-film MBM diodes with good long-term stability have recently been developed [14]. These thin-film diodes have rectangular cross sections, as was assumed in this paper. Coupling of the signal into and out of the diode can be facilitated by forming a dielectric waveguide in the buffer layer formed when constructing the diode [14]. However, no thin-film MBM diodes constructed to date have exhibited negative differential resistance in their current–voltage characteristics, because at the bias potentials required for negative resistance the resulting current densities are so large that the thin-film diodes burn out [15]. More developmental work must be done on these new thin-film MBM diodes in order to produce stable diodes exhibiting negative differential resistance in their current–voltage characteristics.

IV. Conclusion

The gain of a simplified model of a point contact MBM diode with a negative differential resistance region in its static I–V characteristic was derived by treating the diode as a transmission line. It was shown theoretically that an MBM diode amplifier could produce useful gain (approximately 6 dB) with a frequency response of less than 1.5 dB over a decade frequency range in the near infrared.

It should be noted that in order to obtain a value for the differential tunneling conductance per unit length on the order of 10^6 S/m with MBM diodes that have been successfully produced in the laboratory would require biasing the diode very close to the knee of the I–V characteristic curve [3]–[4]. At this bias point only very small signals could be amplified without distortion. Bias stability would probably prove to be a major problem,

since a small change in bias would result in a large change in g_t and, as can be seen from Fig. 3, a large change in G. Much more theoretical and experimental work must be done in order to produce MBM diodes with high values of negative differential tunneling conductance and reasonable bias stability.

Appendix

As given by Jordan and Balmain [8], the method of analysis by which the transmission line parameters are determined from the electric and magnetic fields of the guiding structure assumes there is no penetration of the fields into the metal surfaces. If the fields do not penetrate the surface, the transmission line current must exist on the surface only. This surface current is given by

$$I_S = \int_C \bar{H} \cdot d\bar{l} \tag{A1}$$

where the path of integration C is taken along the metal surface, from one side of the guiding structure to the other, perpendicular to the flow of energy. In the case of this paper, the curve C would be found at $x = d$, from $y = +b$ to $y = -b$.

However, for the surface waves considered in this paper, the fields do penetrate the metal surfaces, so the transmission line current is not a surface current. Therefore, from Maxwell's equation for the curl of the magnetic field intensity, the current is given by

$$I = \int_S (\bar{\nabla} \times \bar{H}) \cdot d\bar{S} \tag{A2}$$

where the oriented surface $\bar{S}$ extends from the surface of the metal to infinity. The normal to $\bar{S}$ is parallel to the energy flow. In the case considered in this paper, the normal to $\bar{S}$ would point in the positive z direction.

For the surface waves and guiding structure considered in this paper, the magnetic field intensity in the region $x \geq d$ has the form

$$H_y = E_0 \frac{\omega \epsilon_b}{k} (G_1 e^{\delta b^d} - G_2 e^{-\delta b^d}) e^{-\delta I^{(x-d)}}. \tag{A3}$$

Now apply Stoke's theorem to the right side of (A2), yielding

$$I = \int_b^{-b} H_y|_{x=d} dy + \int_d^{\infty} H_y|_{y=-b} dx + \int_{-b}^{b} H_y|_{x=\infty} dy + \int_{\infty}^{d} H_y|_{y=b} dx. \tag{A4}$$

Note that in this case, since there is no variation in the y direction, the second and fourth terms on the right side of (A4) cancel each other. Also, from (A3), it can be seen that the third term on the right side of (A4) is zero, since the magnetic field disappears at $x = \infty$. Equation (A4) has been reduced to

$$I = \int_b^{-b} H_y|_{x=d} dy.$$

This is equivalent to (A1), thus proving that the method of [8] can be applied to the analysis of this paper.

References

[1] S. M. Faris, T. K. Gustafson, and J. C. Wiesner, "Detection of optical and infrared radiation with dc-biased electron-tunneling metal–barrier–metal diodes," *IEEE J. Quantum Electron.*, vol. QE-9, pp. 737–745, July 1973.

[2] E. Sakuma and K. M. Evenson, "Characteristics of tungsten–nickel point contact diodes used as laser harmonic-generator mixers," *IEEE J. Quantum Electron.*, vol. QE-10, pp. 509–603, Aug. 1974.

[3] S. Y. Wang, S. M. Faris, D. P. Siu, R. K. Jain, and T. K. Gustafson, "Enhanced optical frequency detection with negative differential resistance in metal–barrier–metal point-contact diodes," *Appl. Phys. Lett.*, vol. 25, pp. 493–495, Nov. 1974.

[4] D. P. Siu, R. K. Jain, and T. K. Gustafson, "Stimulated electron tunneling in metal–barrier–metal structures due to surface plasmons," *Appl. Phys. Lett.*, vol. 28, pp. 407–410, Apr. 1976.

[5] L. M. Matarrese and K. M. Evenson, "Improved coupling to infrared whisker diodes by use of antenna theory," *Appl. Phys. Lett.*, vol. 17, pp. 8–10, July 1970.

[6] D. P. Siu and T. K. Gustafson, "Coherent coupling of radiation to metal–barrier–metal structures by surface plasmons," *Appl. Phys. Lett.*, vol. 31, pp. 71–73, July 1977.

[7] E. N. Economou, "Surface plasmons in thin films," *Phys. Rev.*, vol. 182, pp. 539–554, June 1969.

[8] E. C. Jordan and K. G. Balmain, *Electromagnetic Waves and Radiating Systems*, 2nd ed. Englewood Cliffs, NJ: Prentice-Hall, 1968, pp. 208–209.

[9] J. Schoenwald, E. Burstein, and J. M. Elson, "Propagation of surface polaritons over macroscopic distances at optical frequencies," *Solid-State Commun.*, vol. 12, pp. 185–189, 1973.

[10] S. I. Green, "Point contact MOM tunneling detector analysis," *J. Appl. Phys.*, vol. 42, pp. 1166–1169, Mar. 1971.

[11] H. B. Dwight, *Tables of Integrals and Other Mathematical Data*, 4th ed. New York: MacMillan Co, 1961, pp. 79–87.

[12] S. M. Sze, *Physics of Semiconductor Devices*, New York: Wiley-Interscience, 1969, p. 591.

[13] J. G. Simmons, "Electric tunnel effect between dissimilar electrodes separated by a thin insulating film," *J. Appl. Phys.*, vol. 34, pp. 2581–2590, Sept. 1963.

[14] M. Heiblum, S. Wang, J. R. Whinnery, and T. K. Gustafson, "Characteristics of integrated MOM junctions at dc and at optical frequencies," *IEEE J. Quantum Electron.*, vol. QE-14, pp. 159–169, Mar. 1978.

[15] T. K. Gustafson, private communication.

[16] T. K. Ishii, *Microwave Engineering*. New York: Ronald Press, 1966.